Eur. Phys. J. D **7**, 219–227 (1999)

**THE EUROPEAN PHYSICAL JOURNAL D**

EDP Sciences


# Temperature and size dependence of the optical response of small $Ag_n$ clusters

T. Zabel[1], M.E. Garcia[2,a], and K.H. Bennemann[1]

[1] Institut für Theoretische Physik, Freie Universität Berlin, Arnimallee 14, 14195 Berlin, Germany
[2] Max-Born-Institut, Rudower Chaussee 6, 12489 Berlin, Germany

Received: 4 January 1999 / Received in final form: 12 May 1999

**Abstract.** The absorption spectra of small $Ag_n^+$ clusters are calculated at finite vibrational temperature by using a microscopic tight-binding RPA method. We consider free clusters with sizes between $n = 3$ and $n = 13$ and take into account explicitly the degrees of freedom corresponding to the $4d$-electrons. We analyze the optical absorption as a function of the cluster size. We show that the contribution of the $d$-electrons has an important influence on the size dependence of the energy of the Mie plasmon. We also perform ensemble averages to obtain the absorption spectra for different vibrational temperatures. We obtain relatively good agreement with experiment for a temperature $T \sim 500$ K. The dynamics of the $4d$-electrons, which shows in small clusters an incipient delocalized character for $n > 7$, yields an important contribution to the absorption spectrum already for $n = 13$. We find that the strength of this contribution can be controlled by varying the vibrational temperature.

**PACS.** 36.40.Vz Optical properties of clusters – 71.15.Fv Atomic- and molecular-orbital methods (including tight binding approximation, valence-band method, etc.) – 31.15.Qg Molecular dynamics and other numerical methods

## 1 Introduction

The size dependence of the optical properties of small clusters has been the subject of many experimental and theoretical studies in the last 15 years [1,2]. Most of the early theoretical investigations focussed on alkali metal clusters, where a jellium-like description was expected to be sufficient, and therefore payed relative little attention to the influence of the atomic structure on the absorption spectra. In the last years, however, it was shown that even for $Na_n$ clusters the ionic cores must be taken into account, either as additional degrees of freedom [3] or as a pseudopotential for the valence electrons [4], in order to achieve a correct description of the electronic and optical properties.

On the basis of such studies it is clear that clusters of any element other than sodium atoms should exhibit an important influence of the atomic structure on the electronic properties and on the absorption spectra. Particularly interesting is the case of systems containing, apart from core electrons, also quasi-core electrons, like the $d$-electrons in noble-metal clusters. For instance, the $4d$-electrons of $Ag_n$ clusters cannot be treated simply as core electrons. These electrons not only serve as polarizable medium which takes active part in the screening of charge fluctuations, but they can also delocalize and form a band. The strong influence of interband transitions involving the $4d$-electrons on the optical properties of bulk-silver manifests itself in the reduction of the plasma frequency with respect to the expected electron-gas value $\omega_{\rm p}^0(\mathbf{q} \to 0) = \sqrt{4\pi e^2 \rho_{\rm e}/m_{\rm e}}$, where $\rho_{\rm e}$ and $m_{\rm e}$ refer to the electronic density and the electron mass, respectively [5]. Also the dispersion of the surface plasmon of silver exhibits an anomalous behavior due to the presence of the $d$-electrons [6,7]. In silver surfaces $\omega_{\rm p}(\mathbf{q}_{||})$ shows a positive dispersion, *i.e.*, it increases monotonically for increasing wave vector $\mathbf{q}_{||}$ near $\mathbf{q}_{||} = 0$, in contrast to what occurs in alkali-metal surfaces, where $\omega_{\rm p}(\mathbf{q}_{||})$ decreases with $\mathbf{q}_{||}$ for $\mathbf{q}_{||} \to 0$ (*i.e.*, shows a negative dispersion [8,9]).

As has been shown recently, there is a correspondence between the dispersion of the surface plasmon for increasing $\mathbf{q}_{||}$) and size dependence of the cluster-plasmon for decreasing size [7,10]. According to this one would expect for $Ag_n$ clusters a blue-shift of the Mie resonance for decreasing size, in contrast to the red-shift observed for $Na_n$ clusters. Tiggesbäumker *et al.* [11–13] have measured the absorption cross-section of free $Ag_n^+$ clusters and confirmed the existence of a blue-shift of $\omega_{\rm p}(n)$ for decreasing $n$ within the size range $20 \leq n \leq 70$. For very small clusters ($5 \leq n \leq 13$) no clear trend for the size dependence of the main resonance can be observed [11–13]. Experimentally determined absorption spectra of neutral $Ag_n$ clusters embedded in rare-gas matrices show a rich

[a] e-mail: garcia@physik.fu-berlin.de

structure and a different size dependence of the Mie resonance with respect to free clusters. Both effects can be attributed to the influence of the matrix, which could favor cluster structures which do not correspond to the energy minimum in the gas phase [14]. The interplay between the influence of the *d*-electrons and atomic structure of the clusters remains an open problem.

From the above-mentioned experimental results it becomes clear that the contribution of the *d*-electrons on the optical properties of noble-metal clusters is a problem of general interest, which needs also a theoretical description. Recently, Serra and Rubio have developed a generalized time-dependent density-functional theory which takes into account core polarization effects in the optical response of metal clusters [15]. They applied this approach to large $Ag_n^+$ clusters ($n > 50$) in the framework of the jellium model and obtained good agreement with experiment. So far, no calculations for small clusters have been performed. Moreover, the question regarding at which cluster size the band character of the 4*d*-electrons starts to influence the absorption spectrum has not been answered yet.

Up to now, no theoretical studies have been performed on the influence of the cluster structure and of the 4*d*-electrons on the optical properties of small silver clusters. Small sizes are particularly interesting, because the structure could play an important role regarding the influence of the *d*-electrons. In different isomers the contribution of *d*-electrons to the optical properties could be different. If this is the case, then the vibrational temperature of the cluster might become an important parameter to control the position of the Mie resonance.

In this paper we study the temperature dependence of the optical properties of small $Ag_n^+$ clusters by combining a microscopic electronic theory with molecular-dynamics simulations. We consider the 4*d*-electrons as additional degrees of freedom and not simply as core electrons. This allows us to determine the contribution of the delocalization of the 4*d*-electrons as a function of the cluster size to the absorption spectrum $\sigma(\omega)$. Since we are able to calculate the absorption spectra for arbitrary cluster structures we also study, for the first time, the ensemble-averaged absorption cross-section $\overline{\sigma}(\omega, T)$ of $Ag_n^+$ clusters as a function of temperature. We show that the contribution of the 4*d*-electrons to the absorption spectra of silver clusters is temperature dependent.

The paper is organized as follows. In sections 2.1 and 2.2 we describe the tight-binding random phase approximation formalism we use to calculate the absorption cross-section of the clusters. In section 2.3 we show how finite vibrational temperatures of the clusters can be included into the calculations. Our results concerning size dependence, temperature dependence and contribution of the 4*d*-electrons and the comparison with experiment are presented in section 3. In section 4 we summarize the results.

## 2 Theory

### 2.1 Hamiltonian

For the description of the electronic system of the $Ag_n$ clusters including the 4*d*-electrons we use a Hamiltonian which consists of attractive terms, represented by a tight-binding Hamiltonian $\hat{H}_{\mathrm{TB}}$, and a potential $\phi_{\mathrm{rep}}$ describing core-core repulsion. The total Hamiltonian reads

$$\hat{H}_{\mathrm{total}} = \hat{H}_{\mathrm{TB}} + \sum_{i<j}^{N} \phi_{\mathrm{rep}}(|\mathbf{R}_{ij}|). \tag{1}$$

In equation (1) the tight-binding terms $\hat{H}_{\mathrm{TB}}$ are given by

$$\hat{H}_{\mathrm{TB}} = \sum_{i\alpha} \epsilon_{i\alpha} c_{i\alpha}^{\dagger} c_{i\alpha} + \sum_{\substack{i\alpha j\beta \\ i\neq j}} t_{i\alpha j\beta} c_{i\alpha}^{\dagger} c_{j\beta}, \tag{2}$$

where $c_{i\alpha}^{\dagger}$ ($c_{j\beta}$) refers to the creation (annihilation) operator for an electron at the orbital $\alpha$ of atom $i$. The quantities $\epsilon_{i\alpha}$ stand for the on-site energies. $t_{i\alpha j\beta}$ refer to the hopping integrals between the orbitals $i\alpha$ and $j\beta$, which depend on the distance vector $\mathbf{R}_{ij}$ between atoms $i$ and $j$.

In order to take into account the the resulting angular dependence of $t_{i\alpha j\beta}$ we use the Slater-Koster parameters [16,17]. Following Goodwin *et al.* [18] we write the radial dependence of the *ss*-, *sp*- and *pp*-hoppings as

$$t_{ll'\mu}\left(\frac{R_0}{R_{ij}}\right) = t_{ll'\mu}(1)\left(\frac{R_0}{R_{ij}}\right)^{n_{\mathrm{h}}} \times \exp\left[n_{\mathrm{h}}\left(-\left(\frac{R_{ij}}{r_{\mathrm{c}}}\right)^{n_{\mathrm{c}}} + \left(\frac{R_0}{r_{\mathrm{c}}}\right)^{n_{\mathrm{c}}}\right)\right], \tag{3}$$

where $n_{\mathrm{h}}$ is the hopping exponent. $R_0$ refers to the equilibrium interatomic distance, whereas $n_{\mathrm{c}}$ and $r_{\mathrm{c}}$ are the cut-off exponent and the cut-off radius, respectively [18]. For the distance dependence of the *dd*-, *sd*- and *pd*-hoppings we used the approach proposed by Harrison [17]. In equation (1) the distance dependence of the potentials corresponding to the core-core interactions is given by [18]

$$\phi_{\mathrm{rep}}\left(\frac{R_0}{R_{ij}}\right) = \phi(1)\left(\frac{R_0}{R_{ij}}\right)^{n_{\mathrm{r}}} \times \exp\left[n_{\mathrm{r}}\left(-\left(\frac{R_{ij}}{r_{\mathrm{c}}}\right)^{n_{\mathrm{c}}} + \left(\frac{R_0}{r_{\mathrm{c}}}\right)^{n_{\mathrm{c}}}\right)\right], \tag{4}$$

where $n_{\mathrm{r}}$ is the exponent which determines the range of the repulsive potential. The cut-off parameters $r_{\mathrm{c}}$ and $n_{\mathrm{c}}$ are the same as in equation (3).

### 2.2 Linear response theory

On the basis of the Hamiltonian presented in 2.1 we consider now the interaction of the cluster with the external field. Conventional time-dependent perturbation theory shows that the frequency-dependent polarizability tensor $\alpha_{\mu\nu}(\omega)$ is expressed by the density-density correlation

function $\chi(\mathbf{r},\mathbf{r}',\omega)$,

$$\alpha_{\mu\nu}(\omega) = -e^2 \iint \mathrm{d}^3r\,\mathrm{d}^3r'\,r^{\nu}\,r'^{\mu}\,\chi(\mathbf{r},\mathbf{r}',\omega)\,. \quad (5)$$

In order to determine $\chi(\mathbf{r},\mathbf{r}',\omega)$ we use the RPA expansion

$$\chi(\mathbf{r},\mathbf{r}',\omega) = \chi_0(\mathbf{r},\mathbf{r}',\omega) + \iint \mathrm{d}^3r''\mathrm{d}^3r'''\chi_0(\mathbf{r},\mathbf{r}'',\omega)V(\mathbf{r}'',\mathbf{r}''')\chi(\mathbf{r}''',\mathbf{r}',\omega)\,, \quad (6)$$

where $V(\mathbf{r},\mathbf{r}') = e^2/|\mathbf{r}-\mathbf{r}'|$ is the Coulomb interaction between the electrons. $\chi_0(\mathbf{r},\mathbf{r}',\omega)$ is the single-particle susceptibility, which is obtained after diagonalizing $H_{\mathrm{total}}$ and is given by

$$\chi_{0j\gamma\delta}^{i\alpha\beta} = \sum_{kk'\sigma}(f_k - f_{k'})\frac{a_{i\alpha}^k a_{i\beta}^{k'} a_{j\gamma}^k a_{j\delta}^{k'}}{\hbar\omega - (E_{k'}-E_k) + i\Gamma}\,, \quad (7)$$

where $E_k$ are the single-particle (tight-binding) eigenenergies and $f_k$ are the corresponding Fermi occupation functions. The quantities $a_{i\alpha}^k$ are the coefficients for the expansion $\psi_k(\mathbf{r}) = \sum_{i\alpha} a_{i\alpha}^k \varphi_{i\alpha}(\mathbf{r})$ of the eigenfunctions $\psi_k(\mathbf{r})$ in terms of the local orbitals.

We express the general self-consistent equation (6) in our atomic basis set underlying the tight-binding Hamiltonian of equations (2). For this purpose we expand $\chi(\mathbf{r},\mathbf{r}',\omega)$ in terms of the local basis functions $\varphi_{i\alpha}(\mathbf{r}) = \varphi_\alpha(\mathbf{r}-\mathbf{R}_i)$ as

$$\chi(\mathbf{r},\mathbf{r}',\omega) = \sum_{\substack{i\alpha\beta\\ j\gamma\delta}} \chi_{j\gamma\delta}^{i\alpha\beta}\,\varphi_{i\alpha}^*(\mathbf{r})\,\varphi_{i\beta}(\mathbf{r})\,\varphi_{j\gamma}(\mathbf{r}')\,\varphi_{j\delta}^*(\mathbf{r}')\,, \quad (8)$$

where $i$ and $j$ refer to the atomic sites, $\alpha,\beta,\gamma$ and $\delta$ to the corresponding local orbitals. A similar expansion is performed for $\chi_0(\mathbf{r},\mathbf{r}',\omega)$. If we insert the expansions into the self-consistent equation, we obtain the following matrix equation [19,20]:

$$\chi_{j\gamma\delta}^{i\alpha\beta} = \chi_{0j\gamma\delta}^{i\alpha\beta} + \sum_{\substack{i'\alpha'\beta'\\ j'\gamma'\delta'}} \chi_{0j'\gamma'\delta'}^{i\alpha\beta}\; V_{j'\gamma'\delta'}^{i'\alpha'\beta'}\; \chi_{j\,\gamma\delta}^{i'\alpha'\beta'}\,, \quad (9)$$

where $V_{j\gamma\delta}^{i\alpha\beta}$ is the Coulomb-interaction matrix in the local representation,

$$V_{j\gamma\delta}^{i\alpha\beta} = \iint \mathrm{d}^3r\mathrm{d}^3r'\frac{e^2}{|\mathbf{r}-\mathbf{r}'|} \times\varphi_{i\alpha}^*(\mathbf{r})\varphi_{i\beta}(\mathbf{r})\varphi_{j\gamma}(\mathbf{r}')\varphi_{j\delta}^*(\mathbf{r}')\,. \quad (10)$$

The density-density correlation function $\hat{\chi}(\omega)$ in the local matrix representation is thus obtained by solving equation (9) as

$$\hat{\chi}(\omega) = [1-\hat{\chi}_0(\omega)\hat{V}]^{-1}\,\hat{\chi}_0(\omega)\,, \quad (11)$$

where $\hat{\chi}_0(\omega)$ refer to the single-particle susceptibility in matrix form and $\hat{V}$ to the Coulomb interaction matrix.

The matrix $\hat{\chi}(\omega)$ contains information about the electronic excitations of the cluster and can be used to calculate the absorption spectrum. The polarizability tensor can be expressed in terms of local basis set as

$$\alpha_{\mu\nu}(\omega) = -e^2 \sum_{i\alpha\beta j\gamma\delta} r_{i\alpha\beta}^{\mu}\,r_{j\gamma\delta}^{\nu}\,\chi_{j\gamma\delta}^{i\alpha\beta}(\omega)\,, \quad (12)$$

where $r_{i\alpha\beta}^{\mu}$ refers to the $\mu$ component of the dipole matrix element

$$\mathbf{r}_{i\alpha\beta} = \int \mathrm{d}^3r\,\mathbf{r}\;\varphi_\alpha(\mathbf{r}-\mathbf{R}_i)\;\varphi_\beta(\mathbf{r}-\mathbf{R}_i)\,. \quad (13)$$

In order to compare with experimental results one has to take into account that clusters are randomly oriented in the cluster beam. Therefore we determine the average polarizability which is given by

$$\langle\alpha(\omega)\rangle = \frac{1}{3}\sum_{\mu=1}^{3}\alpha_{\mu\mu}(\omega)\,. \quad (14)$$

Using Fermi's Golden Rule the absorption cross-section $\sigma(\omega)$ can be written as

$$\sigma(\omega) = 4\pi\frac{\omega}{c}\,\mathrm{Im}\langle\alpha(\omega)\rangle\,. \quad (15)$$

### 2.3 Finite temperatures

The theory described in sections 2.1 and 2.2 can account for the optical response of clusters at zero temperature. However, in most experiments clusters are at a finite vibrational temperature. Thus, comparison with experiment requires to take into account temperature effects. This can be achieved by combining the RPA calculations for $\sigma(\omega)$ with Born-Oppenheimer molecular-dynamics simulations.

Diagonalization of the total Hamiltonian $H_{\mathrm{total}}$ allows us the determination of the total energy of the cluster $E_{\mathrm{total}}(\{\mathbf{R}_i\})$, which is a function of atomic coordinates $\{\mathbf{R}_i\}$ and determines a potential energy surface for the atomic motion. Therefore, one can calculate the force $\mathbf{F}_l$ acting on atom $l$ as

$$\mathbf{F}_l = -\nabla_l\,E_{\mathrm{total}}(\{\mathbf{R}_i\})\,. \quad (16)$$

For the calculation of the derivatives of $E_{\mathrm{total}}$ we make use of the Hellmann-Feynman theorem. Thus, the $\nu$ component of the force $\mathbf{F}_l$ is written as

$$F_l^{\nu} = -\sum_{k}^{\mathrm{occupied}}\langle k|\frac{\partial\hat{H}_{\mathrm{TB}}}{\partial R_l^{\nu}}|k\rangle - \sum_{i<j}^{N}\frac{\partial\phi_{\mathrm{rep}}(|\mathbf{R}_{ij}|)}{\partial R_l^{\nu}}\,, \quad (17)$$

where the sum in the first term runs over the occupied eigenstates of $\hat{H}_{\mathrm{TB}}$ and $\langle k|\partial\hat{H}_{\mathrm{TB}}/\partial R_l^{\nu}|k\rangle$ refers to the expectation value of the derivatives of $\hat{H}_{\mathrm{TB}}$ in the tight-binding states $|k\rangle$.

We treat the dynamics of the atoms classically and solve the equations of motions by using the Verlet integrator.

In order to simulate finite temperatures we generate, for each size, a distribution of $\sim 10^3$ clusters having a given average kinetic energy $\overline{E}_{\rm kin}$. For this purpose we proceed in the following way [21]. First, we perform an initialization of the velocities of the atoms so that they are approximately described by a Boltzmann-Maxwell distribution. Then, by repeated scaling of the velocities the cluster is given a certain amount of internal energy. Finally, the cluster evolves freely over a long time $\tau \simeq 10^6$ time steps, exploring the phase space accessible to this internal energy. The time step used in the molecular-dynamics simulations was $\Delta t = 5 \cdot 10^{-16}$ s. Thus, the length of the trajectories was $10^4 \omega_{\rm D}^{-1}$, where $\omega_{\rm D} = 2.94 \cdot 10^{13} {\rm s}^{-1}$ is the Debye frequency of bulk Ag. Representative points of the phase space (structures and velocities) are picked up to form the desired ensemble, whose temperature $T$ is given by [21]

$$T = \frac{2}{(3N-6)} \frac{\overline{E}_{\rm kin}}{k_{\rm B}}, \tag{18}$$

where $k_{\rm B}$ is the Boltzmann constant, and $\overline{E}_{\rm kin}$ the time average of the kinetic energy over the long MD run. The factor $3N-6$ results from the conservation of the total linear and angular momenta in the MD simulations. Making use of the ergodic theorem one can thus express the average cross-section $\overline{\sigma}(\omega, T)$ for the cluster ensemble at temperature $T$ as [22]

$$\overline{\sigma}(\omega, T) = \frac{1}{\tau} \int_0^\tau {\rm d}t \; \sigma(\omega)_t, \tag{19}$$

where $\sigma(\omega)_t$ is the partial absorption cross-section of the cluster at the time $t$ during the long simulation.

The procedure used for generating the cluster ensembles at $T \neq 0$ is a standard one, already used to describe phase transitions and temperature dependence of different properties of small clusters in the gas phase [21]. It is important to stress that in order to compare with experiments performed on clusters in the gas phase, the calculation of the optical properties must be done on free clusters, not coupled to any external source of heat (or thermostat). Since the density of clusters in the beam is low, clusters undergo very few collisions and therefore it is more realistic to assume that the temperature of the cluster fluctuates. The method used here is based on this assumption.

The values for the tight-binding parameters and the radial part of the atomic dipole matrix elements used for the calculations are listed in Table 1. Note that the dipole matrix elements defined in equation (13) can be written as $\mathbf{r}_{i\alpha\beta} = \mathbf{d}_{\alpha\beta} + \mathbf{R}_i \delta_{\alpha\beta}$, where the atomic dipole matrix element $\mathbf{d}_{\alpha\beta}$ can be expressed as a product of a radial part $d^{\rm rad}_{\alpha\beta}$ and an angular part $\mathbf{d}^{\rm ang}_{\alpha\beta}$. The values of $d^{\rm rad}_{sp}$ and $d^{\rm rad}_{pd}$ given in Table 1 were obtained from reference [23].

For the hopping elements and on-site energies involving $s$- and $p$-electrons, as well as the values for the cut-off radius and exponents we used the values obtained in reference [24]. This set of parameters was determined to reproduce the equilibrium bond lengths of $Ag_2^-$, $Ag_2$ and $Ag_2^+$.

**Table 1.** Tight-binding parameters and dipole matrix elements used for the present calculations.

| | | | |
|---|---|---|---|
| On-site energies | | | |
| $\epsilon_p - \epsilon_s$ | 3.72 eV | $\epsilon_d - \epsilon_s$ | −4.6 eV |
| Hopping elements | | | |
| $t_{ss\sigma}$ | −0.89 eV | $t_{pd\sigma}$ | −0.46 eV |
| $t_{sp\sigma}$ | 0.95 eV | $t_{pd\pi}$ | 0.21 eV |
| $t_{pp\sigma}$ | 1.49 eV | $t_{dd\sigma}$ | −0.43 eV |
| $t_{pp\pi}$ | −0.42 eV | $t_{dd\pi}$ | 0.23 eV |
| $t_{sd\sigma}$ | −0.49 eV | $t_{dd\delta}$ | 0.0 eV |
| Cut-off parameters | | | |
| $R_0$ | 2.89 Å | $r_{\rm c}$ | 4.33 Å |
| $n_{\rm h}$ | 2 | $n_{\rm c}$ | 2 |
| $n_{\rm r}$ | 5.965 Å | $\phi(1)$ | 0.605 eV |
| Radial dipole matrix elements | | | |
| $d^{\rm rad}_{sp}$ | 1.95 Å | $d^{\rm rad}_{pd}$ | 0.33 Å |
| Damping parameter | | | |
| $\Gamma$ | | | 0.1 eV |

The set of parameters also yield excellent agreement with *ab initio* calculations [25] for the ground-state geometries of $Ag_3^-$, $Ag_3$ and $Ag_3^+$ [24].

For the hopping elements involving the 4*d*-orbitals we used the values given by Harrison in reference [17].

In order to calculate the Coulomb matrix elements, we have used the two-center approximation and we have performed the usual multipole expansion for the Coulomb interactions [19,20]. Thus, in our calculations we consider the direct and exchange intra-atomic Coulomb interactions as well as interatomic charge-charge, charge-dipole and dipole-dipole interactions. For the direct intra-atomic Coulomb interactions we considered $U_{sp} = U_{pp} = U_{ss} = U_{sd} = U_{pd} = U$ and used $U = 7.2$ eV [26]. We determined $U_{dd} = 12.8$ eV and the exchange integrals $J_{\alpha\beta}$ ($J_{sp} = 0.6$ eV and $J_{d\mu d\nu} = 3.3$ eV) from atomic data [27].

The time step used in our simulations ensured, after $10^6$ MD steps, total energy conservation up to $10^{-7}$ eV for $Ag_5^+$, up to $10^{-5}$ eV for $Ag_7^+$ and $Ag_9^+$ and up to $10^{-4}$ eV for $Ag_{13}^+$ .

First we have analyzed the influence of the Coulomb interactions by comparing the single-particle susceptibility $\hat{\chi}_0(\omega)$ and the RPA susceptibility $\hat{\chi}(\omega)$. As expected, it comes out that correlations between electrons cannot be neglected, and $\hat{\chi}_0(\omega)$ does not describe properly the response of the clusters to an external field. Therefore the following results refer always to the RPA susceptibility.

## 3 Results

In this section we present the results of our calculations of the size- and temperature-dependence of the optical response of small $Ag_n^+$ clusters using the theory outlined in section 2.

### 3.1 Absorption spectra at T = 0

For the analysis of $\sigma(\omega)$ at zero vibrational temperature only the contribution of the ground-state structures have to be considered for the calculation of $\hat{\chi}(\omega)$ and $\sigma(\omega)$. In order to determine the ground-state structures of $Ag_n^+$ clusters we performed simulated annealing in the framework of the molecular-dynamics simulations described in section 2. As expected, the ground-state geometries do not change upon variation (at least up to 30%) of the parameters involving $d$-electrons. This is because the $d$ orbitals are full and lie some eV below the highest occupied state. The calculated ground-state structures of $Ag_n^+$ with $n = 5, 7, 9$ and 13 are shown in the inset of Figure 1. Note that we obtained reasonable agreement with the geometries determined with the help of *ab initio* calculations [25].

Figure 1 shows the calculated photoabsorption spectra $\sigma(\omega)$ of $Ag_n^+$ clusters with $n = 5, 7, 9$ and 13. The corresponding atomic structures in the electronic ground state are shown in the inset figures. In the case of $n = 13$ and for the sake of comparison we also show the single-particle absorption cross-section $\sigma^0(\omega)$. It was calculated directly from the single-particle susceptibility (see Eq. (7)) without performing the RPA calculation. $\sigma^0(\omega)$ does not show, of course, any collective effects and therefore gives an idea of the different single-particle transitions contributing to the spectrum. The typical *ss*, *sp* and *pd* transitions are indicated with arrows. Note that no single-particle peak is obtained at 4.4 eV. This is due to the fact that the large peak in the many-body absorption spectrum at this energy corresponds to the plasmon (collective state), which can only be obtained upon including the electron-electron interactions with the help of the PRA procedure. The other peaks of the many-body spectrum (solid line) can be put in correspondence with single-particle transitions.

The main feature common to all cluster sizes is the large resonance (plasmon peak) between 3–4 eV, consistent with experimental results [11–13]. Note, however, that for $Ag_9^+$ we obtain a double-peak structure in the absorption spectrum which is not observed experimentally. With increasing cluster size the frequency of this resonance becomes slightly shifted to higher energies until $n = 9$. For $n = 13$ this shift is reversed. In order to investigate if this effect is caused by the influence of the 4*d*-electrons, it is necessary to determine the 4*d*-contribution to $\sigma(\omega)$.

One of the goals of this paper is to show the importance of the 4*d*-electrons to the optical properties of small $Ag_n^+$ clusters. This can be done by performing a "switch-off" of the contribution of the 4*d*-electrons and compare with the results obtained including that contribution. Within our approach there are two simple ways to achieve this switch off: i) to enlarge considerably the *sd* energy gap by shifting down the on-site energy $\epsilon_d$, which ensures a zero or negligible contribution of the 4*d*-orbitals to interesting frequency region of the optical spectra; ii) to set all hopping elements involving 4*d*-electrons ($t_{dl}$ with $l = s, p_x, p_y, p_z$ and $t_{dd}$) equal to zero. This produces a complete localization of the 4*d*- electrons, which can only contribute to the absorption spectrum through local (intra-atomic) transitions.

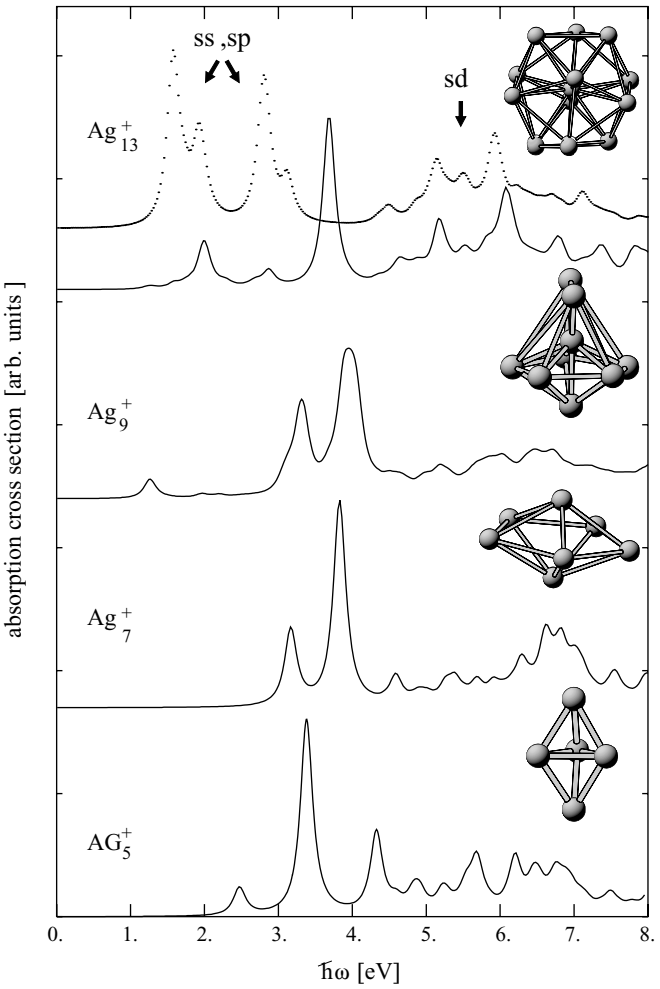


**Fig. 1.** Size dependence of the photoabsorption spectra $\sigma(\omega)$ of $Ag_n^+$ clusters in their ground-state structures (at $T = 0$). The structures have been obtained by simulated annealing on the potential energy surface corresponding to the ground state of the Hamiltonian $\hat{H}_{\text{total}}$ (see text). For comparison we show for $n = 13$ also the single-particle absorption cross-section (dotted line). We also indicate schematically the origin of the absorption peaks for the different single-particle excitation ($s \rightarrow s$, $s \rightarrow p$, $s \rightarrow d$) [21].

In Figures 2 and 3 we show the absorption cross-section of $Ag_5^+$ and $Ag_{13}^+$, respectively, calculated according to the procedures i) and ii) previously described. Comparison of both figures shows that it is not important how the 4*d*-electrons are turned off. Independently of the procedure used for this purpose the main absorption peak is shifted to higher energies. For larger clusters this shift is larger, indicating an increasing influence of the 4*d*-electrons for increasing cluster size.

Thus, from Figures 2 and 3 we conclude that the contribution of the 4*d*-electrons results in a shift of the main resonance to lower frequencies. This result is consistent with the experimentally observed decrease of the

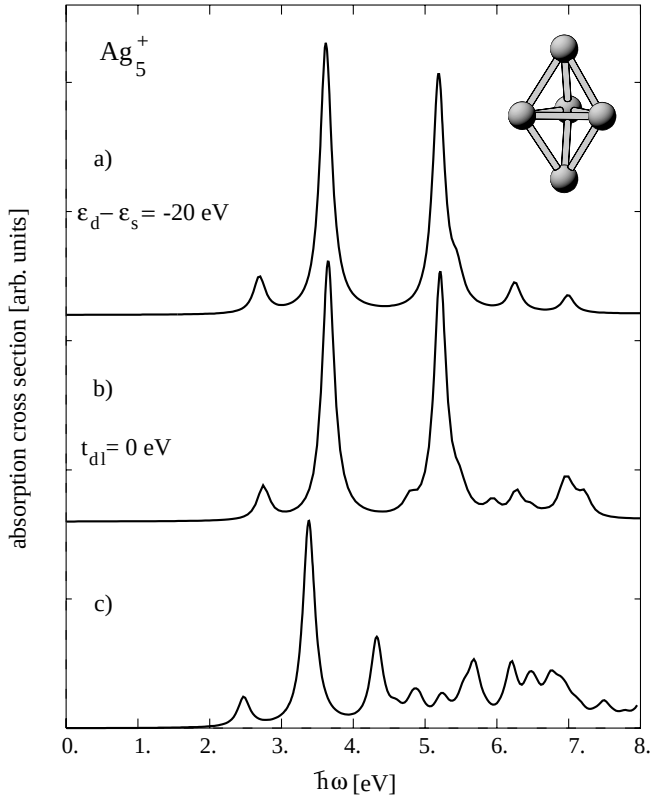


**Fig. 2.** Illustration of the influence of the 4*d*-electrons on the photoabsorption cross-section of $Ag_5^+$ at $T = 0$. In a) and b) the contribution of the 4*d*-electrons is switched off by shifting $\varepsilon_d$ down (a) or by setting all hopping elements $t_{dl}$ with $l = s, p_x, p_y, p_z$ and $d$ equal to zero (b); the subscript $d$ refers to all 5 4*d*-orbitals. In c) the full spectrum including the *d*-electrons is shown. In the inset figure the ground-state structure of $Ag_5^+$ is indicated.

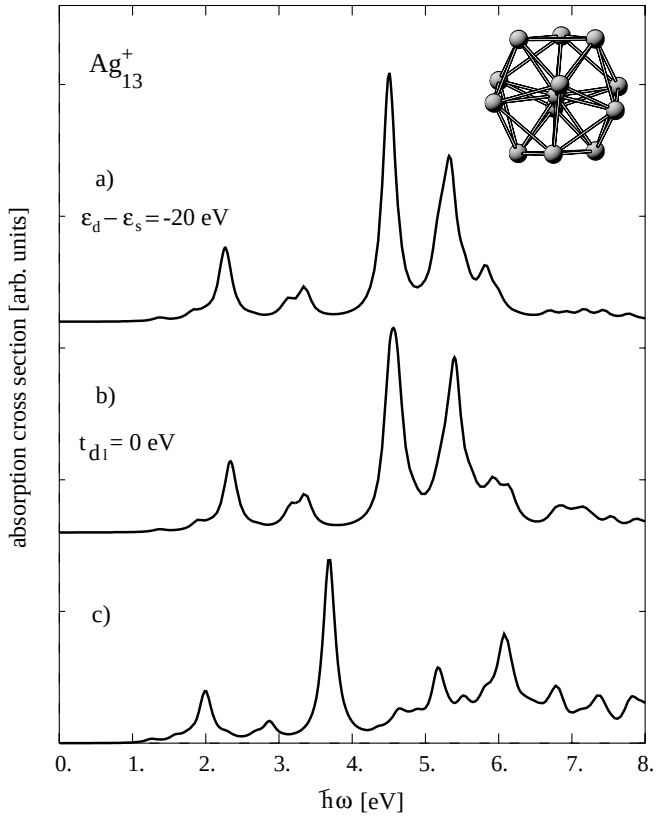


**Fig. 3.** Illustration of the influence of the 4*d*-electrons on the $\sigma(\omega)$ of $Ag_{13}^+$ at $T = 0$, *i.e.* corresponding to the atomic structure in the ground state, shown in the inset figure. For the description of a), b) and c) see caption of Figure 2.

plasma frequency of silver with respect to the free-electron value [5]. For increasing cluster size the degree of delocalization of the 4*d*-electrons increases, the 4*d*-band becomes broader, and the upper 4*d*-states become closer to the Fermi level. As a consequence the contribution of the interband transitions involving 4*d*-orbitals to the total polarizability becomes larger. Therefore, and as is shown in Figures 2 and 3, the blue-shift of the main absorption peak when the *d*-contribution is turned off is larger for $Ag_{13}^+$ than for $Ag_5^+$.

At this stage it is important to comment on the validity of the method used to calculate the absorption cross-section. Since the tight-binding model used in this paper considers only a restricted basis in which, for instance, continuum states are not contained, sum rules are not strictly satisfied. However, as long as the ionization potential of the cluster is larger than the energy of the relevant optical excitations (collective states), continuum states should not have an important influence. This is the case of $Ag_n^+$ clusters. This means that, in the range of energies of the plasmon peak ($\hbar\omega \sim 3$–$4.5$ eV) our method should give qualitatively correct results. For larger energies ($\hbar\omega > 7$ eV), however, the TB-RPA method might give less reliable results. Regarding the stability of the tight-binding parameters used, note that a reasonable variation of the parameters (within $\sim 20\%$) does not produce important changes in the calculated absorption cross-sections.

### 3.2 Absorption spectra at T $\neq$ 0

In this section we present the results obtained by calculating the absorption cross-sections of cluster ensembles at finite temperatures. Recent theoretical and experimental investigations have shown that the vibrational temperature of the cluster leads to a broadening and a redshift of the absorption peaks in small $Na_n$ clusters [22,28, 29]. Thermal broadening of the plasmon linewidth in large clusters has also been theoretically investigated [30–32].

As discussed in section 1, for silver clusters one expects even more interesting temperature effects due to the presence of the 4*d*-electrons.

We used the molecular-dynamics simulation to produce ensembles of clusters of a given cluster size $n$ at a given average temperature $T$ as follows. We first performed the scaling procedure described in section 2. Then, we followed the free evolution of the clusters in their ground-state PES over a time of 20 ps. During this MD

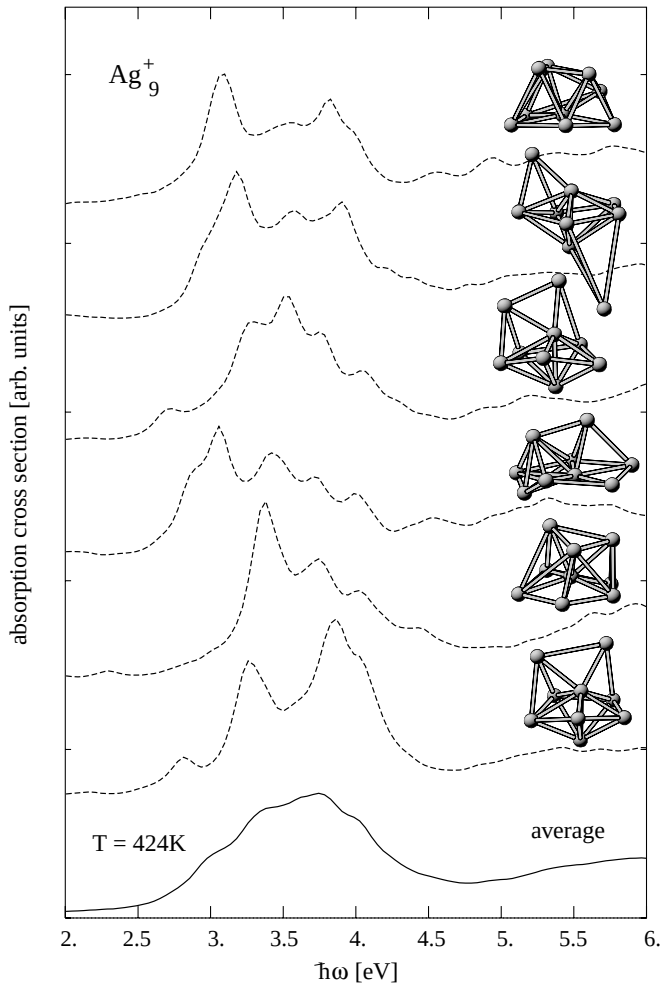


**Fig. 4.** Solid line: average absorption cross-section $\overline{\sigma}(\omega, T)$ of $Ag_9^+$ at a finite temperature $T = 424\,\mathrm{K}$ (solid line). The different curves with dashed lines refer to partial absorption spectra $\sigma(\omega)_t$ (see Eq. (19)) corresponding to different structures present in the cluster ensemble at $T = 424\,\mathrm{K}$ (see text).

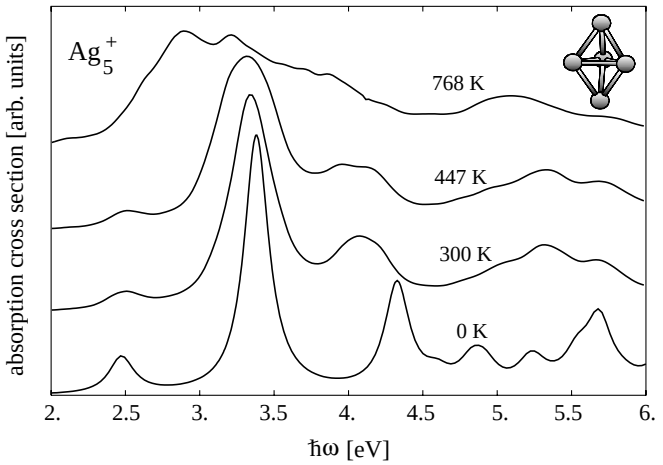


**Fig. 5.** Temperature dependence of the ensemble-averaged absorption cross-section $\overline{\sigma}(\omega, T)$ of $Ag_5^+$. The inset refers to the structure used for $T = 0$ (ground-state structure).

run we picked up 30 representative structures, accessible to the system at the temperature $T$. Then, we calculated for each of these structures the photoabsorption spectra. Finally we determined the averaged spectrum, by approximating the time average in equation (19) by an average over the representative structures.

Figure 4 illustrates the temperature effect on the photoabsorption spectra for $Ag_9^+$ cluster.

In the insets of Figure 4 we show some of the structures considered. As explained above, the average of all these spectra gives the photoabsorption spectrum at the temperature $T = 424\,\mathrm{K}$ determined by equation (18). The figure shows clearly, that there is a strong dependence of the absorption cross-section on the cluster structure. Although all structures explored by the $Ag_9^+$ clusters at $T = 424\,\mathrm{K}$ show a large absorption cross-section for photon frequencies mainly between 3 eV and 4.5 eV there are remarkable differences in the number and strength of the different absorption peaks. The sensitivity of the absorption cross-section to the cluster geometry was already pointed out by Bonacic-Koutecky *et al.* [33]. They have shown that the absorption spectrum can be considered as a fingerprint of the cluster.

In Figure 5 we present results for the photoabsorption spectra of the $Ag_5^+$ cluster at different temperatures. The main features are the increasing broadening and shift to lower energies of large resonance with increasing temperature.

Both effects can be attributed to the dependence of the *s*-like tight-binding states upon interatomic distance. As temperature increases, the mean radius of the clusters becomes larger. With increasing mean interatomic distance the splitting between bonding and antibonding *s*-like states becomes smaller, so that the occupied binding states are shifted upwards. On the other hand the distance dependence of the *p*-like states corresponding to the optical transitions with the largest oscillator strength is rather weak. Therefore the gap between *s*-like and *p*-like states is effectively reduced and the absorption peaks become red-shifted.

This argument cannot be used for larger clusters. For increasing cluster size the influence of the 4*d*-electrons becomes more important and has the opposite effect, as is explained below.

The second important temperature effect is the broadening of the absorption peaks. In our calculations this results from the averaging process over different structures exhibiting different photoabsorption spectra. Thus, the absorption spectra shown in Figure 5 correspond to ensembles of clusters.

Figure 6(a) shows our calculated photoabsorption spectra of $Ag_n^+$ clusters with $n = 5, 7, 9, 13$ at $T \sim 500\,\mathrm{K}$. For the sake of comparison we also show, in Figure 6(b), the experimental results by Tiggesbäumker *et al.* [11–13]. Note that the temperature of the clusters in the experiment is not known. However, the absence of sharp peaks

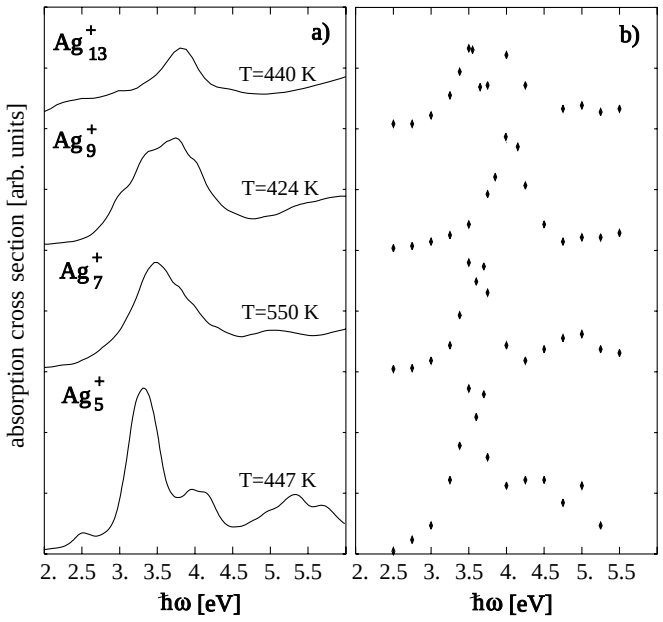


**Fig. 6.** (a) $\overline{\sigma}(\omega, T)$ for different cluster sizes at a temperature $\sim 500$ K. (b) For the sake of comparison, the corresponding experimental spectra obtained by Tiggesbäumker *et al.* (Ref. [12]) are shown.

suggests that the measurements were performed on clusters at high temperatures.

As in the case of $T = 0\,\mathrm{K}$ our spectra exhibit strong resonances between 3 and 4 eV which are now broadened. As mentioned before, the temperature has also the effect to shift the resonance to lower energies for small cluster sizes (see Fig. 5). This is no longer true for the $Ag_{13}^+$ cluster. For this size the resonance is shifted to higher energies, as can be seen by comparing Figure 6(a) with Figure 1 or Figure 3(c).

In order to understand this behavior we have to resort to the results shown in Figure 3. As mentioned above, the main effect of the 4*d*-electrons is to produce, for $n \geq 13$, an appreciable red-shift of the absorption peaks. Now, with increasing temperature the mean atomic spacing increases. Since the fall-off of the hopping elements involving *d*-electrons goes like $\sim 1/r^5$ and $\sim 1/r^{7/2}$, the *d*-contribution to the dynamical polarizability of the cluster becomes rapidly reduced. As a consequence, the blue-shift induced by this reduction dominates over the red-shift due to *s*-band splitting (which goes like $\sim 1/r^2$), and the optical resonance becomes effectively shifted to larger frequencies. This shows that there is an important interplay between cluster structure (and consequently vibrational temperature) and the contribution of the *d*-electrons to the absorption spectrum.

The experimental absorption cross-section of $Ag_{13}^+$ shows two peaks and the main weight is not so far shifted as in our calculation. A possible explanation for this discrepancy might be that the cluster temperature in the experiment is different from 500 K.

It is also important to note that the measured spectra in Figure 6 exhibit sharper features than our calculated ones. By lowering the temperature in our simulations down to room temperature ($\sim 300\,\mathrm{K}$) we can reproduce the widths of the experimental peaks. However, for such temperatures the qualitative agreement with experiment (number of peaks) becomes worse. This could be due to a limitation of our model for the electronic structure. Our model seems to overestimate the sensitivity of the optical properties to structural changes.

As in previous investigations [22,28,29] our results show a broadening of the absorption peaks with increasing temperature. In the cases of $Ag_7^+$ and $Ag_9^+$ our calculated $\sigma(\omega)$ at $T = 0$ shows a double-peak structure which disappears at high temperatures. Experiments at low temperatures should give more information about the form of $\sigma(\omega)$ in the ground-state structures of both clusters.

## 4 Summary and conclusions

In this paper we have analyzed theoretically the size- and temperature-dependence of the ensemble-averaged absorption spectrum $\overline{\sigma}(\omega, T)$ of $Ag_n^+$ clusters. We have calculated explicitly the contribution of the 4*d*-electrons to the optical properties, considering them as additional degrees of freedom of the problem. We have found a strong dependence of the absorption spectrum on the cluster structure, which leads to strong temperature effects. The influence of the 4*d*-electrons to the absorption spectrum increases with cluster size. For $n = 13$ we found an appreciable contribution of the 4*d*-electrons beyond polarization effects, which results in a red-shift of the main absorption peak. Our molecular-dynamics simulations show that the average effective radius of the cluster increases with temperature, and that this leads to a decrease of the influence of the band character of the 4*d*-electrons for high vibrational temperatures.

Note that a similar behavior was experimentally observed in bulk silver by Liljenvall *et al.* [34], who showed that the energy of the peak in the energy loss function between 3.5 eV and 4 eV decreases for increasing temperature.

This effect could be used to control the *d*-electron-contribution, and consequently the position of the plasma frequency.

Since the temperature effects are mainly due to the localized character of the *d*-electrons, we expect them to be present also in other noble-metal clusters. In transition metal clusters they might be particularly strong.

We have obtained relatively good agreement with the experimentally determined absorption cross-sections. The method presented in this paper could be used to calculate the optical properties of embedded and adsorbed noble-metal clusters.

This work has been supported by the Deutsche Forschungsgemeinschaft through SFB 337.

## References


1. W.A. de Heer, Rev. Mod. Phys. **65**, 611 (1993).
2. See, for example, *Proceedings of the Eighth International Symposium on Small Particles and Inorganic Clusters ISSPIC 8. Copenhagen, Denmark, 1-6 July 1996*, edited by H.H. Andersen (Springer-Verlag, Berlin, 1997).
3. V. Bonacic-Koutecky, P. Fantucci, J. Koutecky, Chem. Rev. **91**, 1035 (1991).
4. W.-D. Schöne, W. Ekardt, J.M. Pacheco, Phys. Rev. B **50**, 11079 (1994).
5. H. Ehrenreich, H.R. Phillip, Phys. Rev. **128**, 1622 (1962).
6. S. Suto, K.D. Tsuei, E.W. Plummer, E. Burstein, Phys. Rev. Lett. **63**, 2590 (1989).
7. A. Liebsch, Phys. Rev. Lett. **71**, 144 (1993).
8. K.D. Tsuei, E.W. Plummer, A. Liebsch, E. Pehlke, K. Kempa, P. Baskshi, Surf. Sci. **247**, 302 (1991).
9. A.A. Quong, A.G. Eguiluz, Phys. Rev. Lett. **70**, 3955 (1993).
10. Th. Reiners, C. Ellert, M. Schmidt, H. Haberland, Phys. Rev. Lett. **74**, 1558 (1995).
11. J. Tiggesbäumker, L. Köller, H.O. Lutz, K.H. Meiwes-Broer, Chem. Phys. Lett. **190**, 42 (1992).
12. J. Tiggesbäumker, PhD Thesis, University of Bielefeld (1993).
13. J. Tiggesbäumker, L. Köller, K.H. Meiwes-Broer, A. Liebsch, Phys. Rev. A, **48**, R1749 (1993).
14. W. Harbich, S. Fedrigo, J. Buttet, Chem. Phys. Lett. **195**, 613 (1992); S. Fedrigo, W. Harbich, J. Buttet, Phys. Rev. B, **47**, 10706 (1993).
15. Ll. Serra, A. Rubio, Phys. Rev. Lett. **78**, 1428 (1997).
16. J.C. Slater, G.F. Koster, Phys. Rev. **94**, 1498 (1954).
17. W.A. Harrison, Phys. Rev. B **24**, 5835 (1981).
18. L. Goodwin, A.J. Skinner, D.G. Pettifor, Europhys. Lett. **9**, 701 (1989).
19. S. Grabowski, M.E. Garcia, K.H. Bennemann, Phys. Rev. Lett. **72**, 3969 (1994).
20. S. Grabowski, M.E. Garcia, K.H. Bennemann, Mod. Phys. Lett. B **10**, 241 (1996).
21. See, for example, T.L. Beck, J. Jellinek, R.S. Berry, J. Chem. Phys. **87**, 545 (1987).
22. A. Bulgac, C. Lewenkopf, Europhys. Lett. **31**, 519 (1995).
23. S. Fraga, J. Karwowski, K.M.S. Saxena, in *Handbook of Atomic Data* (Elsevier Scientific, Amsterdam, N.Y., 1976); S. Fraga, J. Muszynska, in *Atoms in External Fields* (Elsevier Scientific, Amsterdam, N.Y., 1981).
24. H.O. Jeschke, M.E. Garcia, K.H. Bennemann, Phys. Rev. A **54**, R4601 (1996).
25. V. Bonacic-Koutecky, L. Cespiva, P. Fantucci, J. Koutecky, J. Chem. Phys. **98**, 7981 (1993); V. Bonacic-Koutecky, L. Cespiva, P. Fantucci, J. Pittner, J. Koutecky, *ibid.* **100**, 490 (1994).
26. We have found that the relative values between the different $U_{\alpha\beta}$'s, apart from $U_{dd}$, did not affect the final results for the absorption spectra. Thus, we set $U_{sp} = U_{pp} = U_{ss} = U_{sd} = U_{pd}$ in order to reduce the number of parameters.
27. C. Moore, *Atomic Energy Levels*, Nat. Bur. Stand. Circ. No. 467 (1958).
28. C. Ellert, M. Schmidt, C. Schmitt, T. Reiners, H. Haberland, Phys. Rev. Lett. **75**, 1731 (1995).
29. V. Bonacic-Koutecky, J. Pittner, C. Fuchs, P. Fantucci, M.F. Guest, J. Koutecky, J. Chem. Phys. **104**, 1427 (1996).
30. J.M. Pacheco, R. Broglia, Phys. Rev. Lett. **62**, 1400 (1990); Z. Phys. **D 21**, 289 (1991).
31. Z. Penzar, W. Ekardt, A. Rubio, Phys. Rev. B **42**, 5040 (1990).
32. J.M. Pacheco, W.D. Scöne, Phys. Rev. Lett. **79**, 4986 (1997).
33. See, for example, V. Bonacic-Koutecky, J. Koutecky, M.M. Kappes, P. Fantucci, Chem. Phys. Lett. **170**, 26 (1990).
34. H.G. Liljenvall, A.G. Mathewson, J. Phys. C Suppl. **3**, 341 (1970).